1997

NASA/ASEE SUMMER FACULTY FELLOWSHIP PROGRAM

MARSHALL SPACE FLIGHT CENTER
THE UNIVERSITY OF ALABAMA IN HUNTSVILLE

Controller Design for EMA in TVC Incorporating Force Feedback

Prepared By: Dale E. Schinstock, Ph.D.
and Douglas A. Scott, Accompanying Student

Academic Rank: Assistant Professor

Institution and Department: The University of Alabama
Mechanical Engineering Department

NASA/MSFC:

Laboratory: Propulsion Laboratory
Division: Component Development
Branch: Turbomachinery and Control Mechanisms

MSFC Colleague: Rae Ann Weir (EP32)

Introduction

The objective of this research was to develop control schemes and control design procedures for electromechanical actuators (EMA) in thrust vector control (TVC) applications. For a variety of reasons, there is a tendency within the aerospace community to use electromechanical actuators in applications where hydraulics have traditionally been employed. TVC of rocket engines is one such application. However there is considerable research, development, and testing to be done before EMA will be accepted by the community at large for these types of applications. Besides the development of design procedures for the basic position controller, two major concerns are dealt with in this research by incorporating force feedback: 1) the effects of resonance on the performance of EMA-TVC-rocket-engine systems, and 2) the effects of engine start transients on EMA. This report only highlights the major contributions of this research.

Hardware and Modeling

Experimental verification of the control schemes and design techniques were completed using the 1 Hp EMA designed and built by the Component Development Division of the Propulsion Laboratory at NASA MSFC. It was designed to operate with an engine roughly the size of an RL-10 engine (Pratt and Whitney). The actuator was mounted in an inertia simulator, which is basically a large pendulum used to simulate the engine. Fig.1 shows the hardware used in the experiments. The NASA controller originally included and analog position controller, a motor current controller, and a pulse width modulated power converter for the brushless DC motor in the actuator. For this research, the position controller was defeated and a digital controller was implemented. Using a Pentium™ PC, digital feedback of the screw position from a resolver to digital converter in the NASA controller was utilized for position control of the EMA. Several pieces of hardware are not shown in Fig.1: a string potentiometer for the measurement of the pendulum position, a load cell amplifier, an interface card for the PC, and a large impulse hammer with a piezoelectric load cell and amplifier (PCB GK291B50).

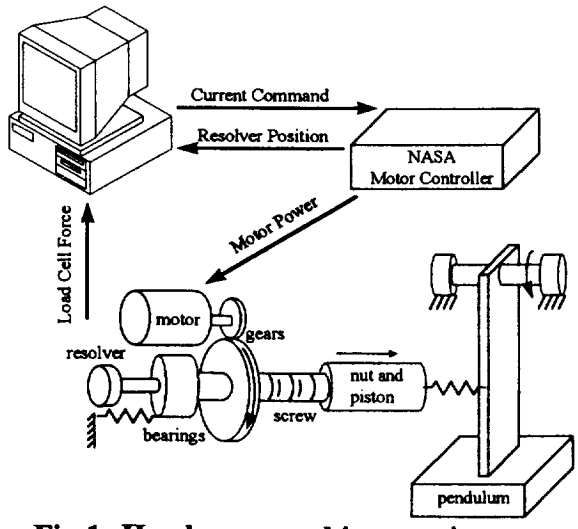

Fig.1: Hardware used in experiments

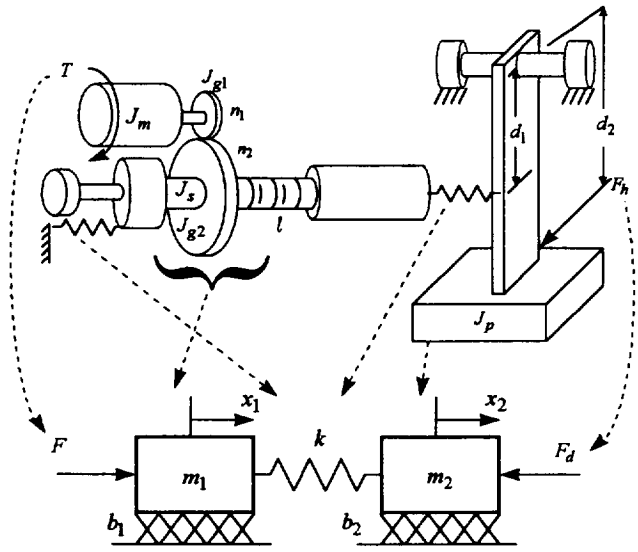

Fig.2: Pictorial of model development

A pictorial representation of the model development is shown in Fig.2. Equations (1) through (5) are necessary for the calculation of some of the model parameters. A linear model of the mechanical system is given in equations (6) through (9).

$$N = n_1 l / (2\pi n_2) \tag{1}$$

$$m_1 = (J_m + J_{g1}) / N^2 + (J_s + J_{g2})(2\pi / l)^2 \tag{2}$$

$$m_2 = J_p / d_1^2 \tag{3}$$

$$F = T / N \tag{4}$$

$$F_d = F_h d_2 / d_1 \tag{5}$$

$$F(s) = (m_1 s^2 + b_1 s + k)X_1(s) - kX_2(s) \tag{6}$$

$$F_d(s) = (m_2 s^2 + b_2 s + k)X_2(s) - kX_1(s) \tag{7}$$

$$\frac{X_1(s)}{F(s)} = \frac{m_2 s^2 + b_2 s + k}{s(m_1 m_2 s^3 + (m_1 b_2 + m_2 b_1)s^2 + (m_1 k + m_2 k + b_1 b_2)s + k(b_1 + b_2))} \tag{8}$$

$$\frac{X_2(s)}{X_1(s)} = \frac{k}{m_2 s^2 + b_2 s + k} \tag{9}$$

Fig. 3 is a block diagram representation of a more complete linear model of the system including the final control architecture chosen after evaluation of several different architectures. The proportional-integral-derivative (PID) position controller and the dynamic force feedback (DFF) compensation filter are implemented digitally in the PC. The force transmitted, $F_t(s)$, through the actuator is measured by the load cell. The DFF filter is similar to the dynamic pressure feedback (DPF) compensation currently used in the controllers for the hydraulic actuators used on the Space Shuttle Main Engines (SSME) (Davis 1973a, Davis 1973b).

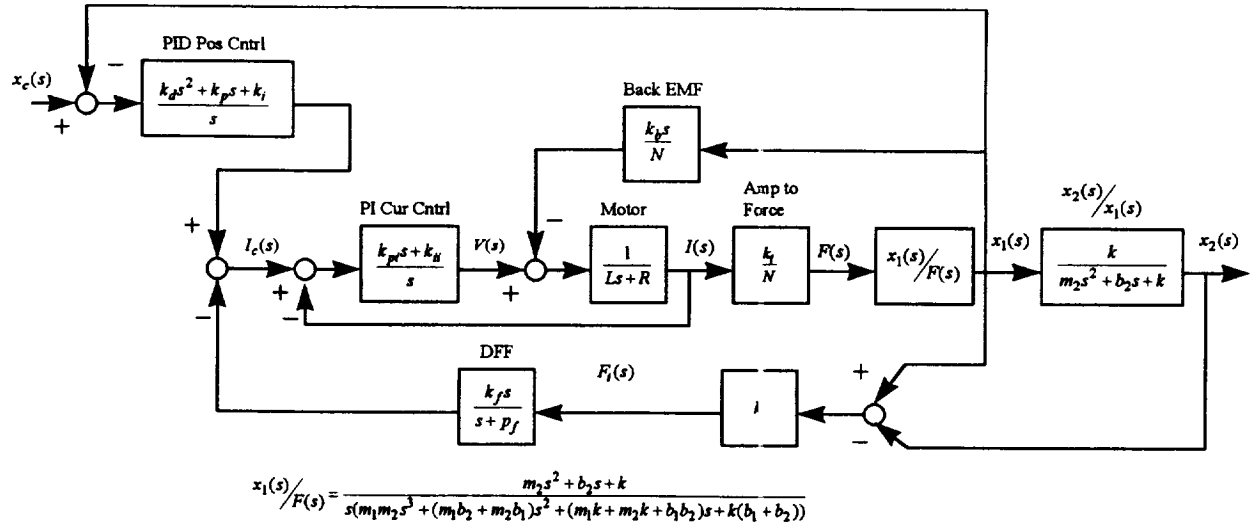

Fig.3: Linear model

Controller Design

A position controller and transmitted force controller have contradictory goals. Therefore, an attempt to simultaneously use two separate compensation loops like the PID controller and the DFF filter in Fig.3 will result in ineffective control of the force and/or the position unless they operate at different frequencies. However, it is advantageous to reduce the undesirable effects of position feedback at resonance. Furthermore, the engine start transient forces occur mainly at the resonant frequency of the system. Therefore, the basic concept of the controller design is to design the position and the force loops separately, with the position loop having good performance at low frequencies and the DFF loop having good performance around the resonance. This is depicted in Fig.4.

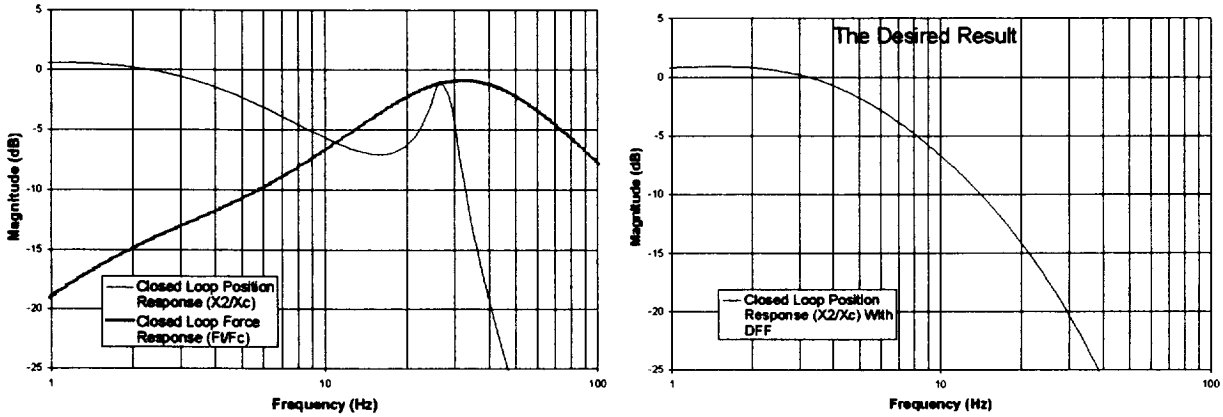

Fig.4: Concept of the control design

The linear model in Fig.3 is reduced slightly for controller design. A simpler model is shown in Fig.5. The electrical dynamics of the current controller and the back emf feedback have been removed. As will be seen in the results, this simplification did not significantly affect the response. Equations (10) through (15) and (16) through (19) are design equations developed for the PID position controller and the DFF filter respectively. These equations should be applied with discretion since every situation will be slightly different. However, they should be a good starting point for any similar design.

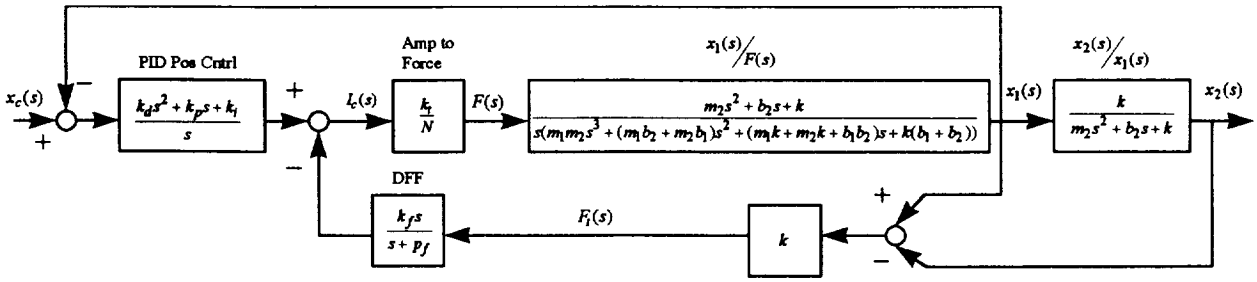

Fig.5: Linear model used in compensation design

$$\omega_{BWp} = 2\pi(\text{Target Position BandWidth in Hz}) \tag{10}$$

$$z_1 = \frac{(b_1 + b_2)}{(m_1 + m_2)} \tag{11}$$

$$z_2 = \frac{\omega_{BWp}}{10} \tag{12}$$

$$k_d = \frac{1}{|G_1(j\omega_{BWp})|} = \sqrt{\frac{{\omega_{BWp}}^4\left((m_1+m_2)N/k_t\right)^2}{{\omega_{BWp}}^2+\left(\omega_{BWp}/10\right)^2}}, \text{ where } G_1(s) = \frac{k_t(s+z_2)}{N(m_1+m_2)s^2} \tag{13}$$

$$k_p = k_d(z_1+z_2) \tag{14}$$

$$k_i = k_d z_1 z_2 \tag{15}$$

$$\omega_{res} = 2\pi(\text{Position Resonance in Hz}) \tag{16}$$

$$p_f = 10\omega_{res} \tag{17}$$

$$\omega_{BWf} = 2\omega_{res} \tag{18}$$

$$k_f = \frac{1}{|G_2(j\omega_{BWf})|} \text{ where } G_2(s) = \frac{k_t k(m_2 s+b_2)s}{N(s+p_f)(m_1m_2s^3+(m_1b_2+m_2b_1)s^2+(m_1k+m_2k+b_1b_2)s+k(b_1+b_2))} \tag{19}$$

Results

The design equations, (10) through (19), were applied to the system used in the experiments. Data for the frequency response of the closed loop position system and for the time response of the transmitted force resulting from hammer impulses was taken. Fig.6 shows the experimentally developed frequency response of the system with and without the DFF compensation. The data points are indicated with dots. The frequency response obtained from the linear model in Fig.5 is also shown. The results are quite encouraging. The DFF reduced the resonant peak by a factor of 10 (20 dB). Furthermore, the models match the actual data fairly well. Similar results were obtained for a 10 Hz position bandwidth design. This reduction in the resonance is a very important result not only because it drastically decreases the magnitude of the forces in the actuator but also because it will result in a more stable subsystem to be used in the control of the dynamic vehicle system.

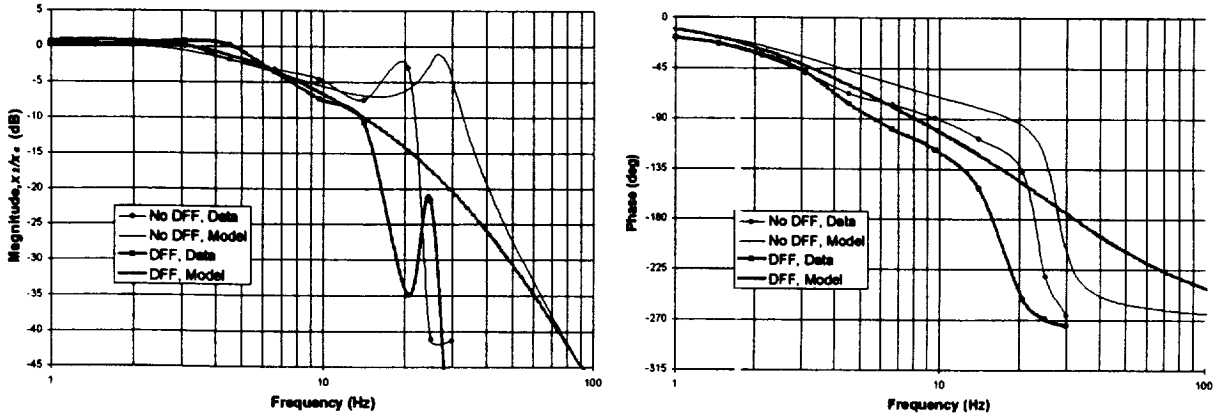

Fig.6: Frequency response of the closed loop position systems w/ 5Hz bandwidth design (0.1 inch amplitude sinusoidal command except at resonance)

Fig.7 illustrates a typical hammer impulse response of the transmitted force. This response is shown along with a simulated response from a nonlinear simulation model constructed in

Simulink™ from Math Works Inc. This model includes all of the dynamics in the linear model shown in Fig.3 and several nonlinear effects such as backlash, static friction, motor current saturation, and voltage saturation. Fig.8 shows some of the experimental data obtained from the many impulse hammer tests conducted. It plots the peak magnitude of the transmitted force versus the area of the hammer impulse. It shows results obtained from several systems: a 10 Hz bandwidth position controller and no DFF, the system with no power applied to the motor controller, a 10 Hz bandwidth position controller with DFF, and a 5 Hz bandwidth position controller with DFF. The DFF significantly reduced the transmitted force. It should therefore reduce the effects of engine start transients on an EMA.

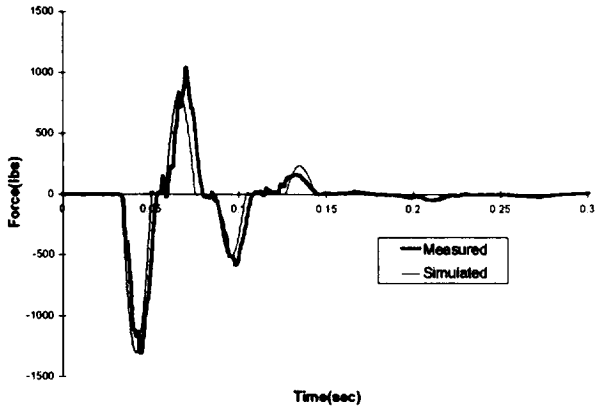

Fig.7: Transmitted force due to a hammer impulse area impulse of 5.8 lb*s; position control only

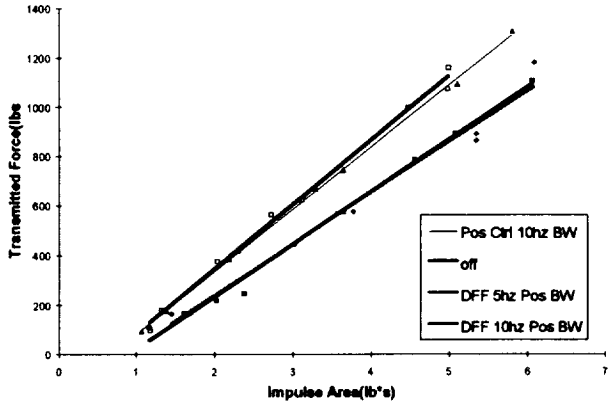

Fig.8: Peak transmitted force vs. hammer

It is reasonable to expect the DFF to reduce the peak force due engine start transients even more than the results in Fig.8. This is because the engine transient forces usually take a few force oscillation cycles to build before they start to decay, unlike the impulse response shown in Fig.7. The forcing function for the transient forces is probably somewhere "in between" an impulse input and driving the position controller at the resonance. At resonance the forces build with time to a large steady state oscillation. By driving the 5 Hz bandwidth position controller without the DFF with a 0.05 in. amplitude sinusoid at resonance, the load cell output is saturated at 2500 lb by the oscillation peaks. However, with the DFF the same input results in a peak amplitude of approximately 600 lb.

References

Davis, M. E. (1973a), *Optimum Gains Determination.* Unpublished report to Mr. C. S. Cornelius, Report No. SP-261-0805 NASA MSFC, October 9,1973.

Davis, M. E. (1973b), *Bulk Modulus and Valve Dynamics Effect on Linear SSME-TVC.* Unpublished report to Mr. C. S. Cornelius, Report No. SP-261-0805-1 NASA MSFC, October 10,1973.